(7) A. Eisner, W. R. Noble, and J. T. Scanlan, *J. Am. Oil Chemists' Soc.*, **36**, 168(1959).
(8) "Chromatography," E. Heftmann, Ed., Reinhold, New York, N. Y., 1961, pp. 428–451.
(9) G. J. Papariello, S. Chulkaratana, T. Higuchi, J. E. Martin, and V. P. Kuceski, *J. Am. Oil Chemists' Soc.*, **37**, 396 (1960).
(10) A. F. Summa and J. H. Graham, *J. Pharm. Sci.*, **54**, 612 (1965).
(11) S. Gottlieb, *J. Am. Pharm. Assoc., Sci. Ed.*, **36**, 379(1947).
(12) L. Lykken, R. S. Treseder, and V. Zahn, *Ind. Eng. Chem. (Anal. Edition)*, **11**, 103(1946).

**ACKNOWLEDGMENTS AND ADDRESSES**

Received April 23, 1969 from the *Drug Standards Laboratory of the American Pharmaceutical Association Foundation, Washington, DC 20037*

Accepted for publication July 9, 1969.

The Drug Standards Laboratory is jointly sponsored by the American Medical Association, the American Pharmaceutical Association, and the United States Pharmacopeial Convention, Inc.

## *TECHNICAL ARTICLES*

# *In Vitro* Assessment of Dissolution Kinetics: Description and Evaluation of a Column-type Method

**F. LANGENBUCHER**

**Abstract** □ A new method is described for the assessment of the dissolution behavior of solid dosage forms. The method, which is based on the mass transfer between solid and liquid phase in an exchange column, is shown to avoid some disadvantages of the commonly used beaker methods employing fixed liquid volumes. Its usefulness is demonstrated by results obtained with nondisintegrating and uniform granules of benzoic acid in water. The influence of various external parameters, such as liquid flow rate, cell cross-sectional area, amount of material, and particle diameter, is found to agree with theory and literature data. Because of its reproducibility and the absence of arbitrary external parameters, the method seems to be useful for a meaningful study of dissolution kinetics.

**Keyphrases** □ Dissolution method—column-type apparatus □ Diagram, dissolution apparatus—column-type □ Kinetics, dissolution—nondisintegrating granules □ Parameters affecting—dissolution kinetics

Most *in vitro* studies reported in the literature on the subject of the dissolution behavior of solid drugs involve modifications of the beaker or stirred-tank model, where the drug is dissolved in a fixed volume of solvent liquid, the agitation being accomplished by means of a stirrer or some rocking or shaking action. These methods in general suffer from several important disadvantages.

1. The flow conditions in the liquid medium depend on a great number of external parameters such as diameter and height of the vessel, liquid volume, speed, position, and form of the stirrer, *etc.* Some of these are difficult to standardize and to reproduce in different laboratories. In addition, the influence of these parameters on the dissolution kinetics is difficult to interpret.

2. The liquid volume must be fixed *a priori*, since it essentially determines the dissolution kinetics. It should be chosen as a standard and in accordance with the *in vivo* conditions. Nevertheless, depending on the solubility and dosage of the drug, variable volumes have been used by different authors: whereas Levy (1) originally proposed 300 ml. as standard, volumes as low as 100 ml. (2, 3) and as large as 2 l. (4, 5) or 20 l. (6) have been used.

3. In all beaker methods the drug concentration in the liquid increases from zero up to either the saturation limit or the concentration which corresponds to the completely dissolved drug amount. This concentration buildup is different from the *in vivo* process in which the dissolved material is removed continuously from the liquid by absorption. Gibaldi and Feldman (7) pointed out that dissolution-limited absorption phenomena must be studied by methods in which the liquid acts as a perfect sink, *i.e.*, the concentration never exeeds 10 to 20% of the saturation. To obtain this, the authors use a sufficiently large reservoir of a water-immiscible organic liquid, which permits the dissolved drug to be removed from the aqueous phase. Other authors attempted to achieve the same objective by means of specific adsorbents in the dissolving liquid (8). Although these modifications reduce the critical role of the aqueous volume, they introduce other arbitrary parameters such as volume

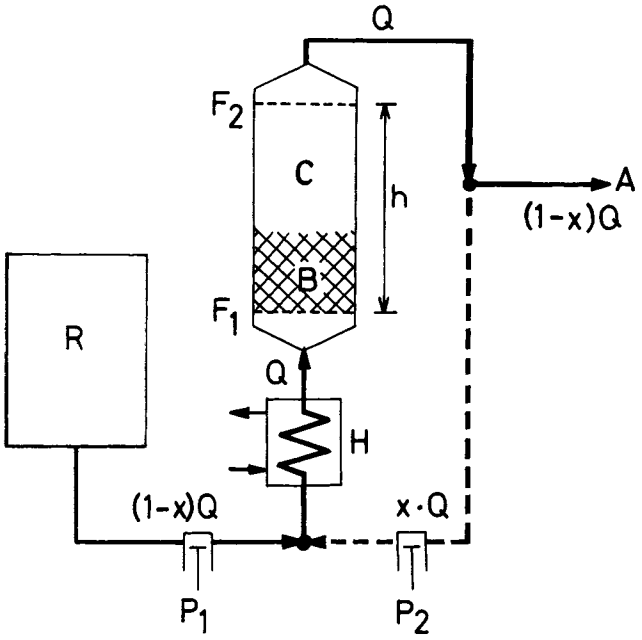


**Figure 1**—*Sketch of the column dissolution apparatus (schematic). Key:* B, *particle bed;* C, *cell;* $F_1$, $F_2$, *screens;* H, *heat exchanger;* h, *height of cell;* $P_1$, $P_2$, *volumetric pumps;* R, *liquid reservoir;* x, *circulation factor;* Q, xQ, (1-x) Q, *volumetric flow rates.*

of organic phase, amount of adsorbent, miscibility of aqueous and organic phase, and solubility of the drug in the two saturated phases.

In this paper another approach is presented, one which is easier to standardize with laboratory equipment and which involves no arbitrary and material-dependent parameters. It is based on the mass transfer in a fixed bed of drug material traversed by a continuous flow of solvent liquid in a vertical-exchange column. Processes of this type have been extensively studied in the field of chemical engineering (9–12). In a recent paper (13), Pernarowski *et al.* also described a continuous-flow apparatus, but in their model agitation again is accomplished by a basket-stirrer assembly which is open to the above-mentioned limitations.[1]

## DESCRIPTION OF THE METHOD

**Basic Design**—The design of the apparatus is shown in Fig. 1. The material to be investigated (tablet, capsule, granules) is placed in the vertically mounted dissolution cell $C$, on a screen $F_1$ which permits fresh solvent to enter from the bottom. $F_1$ is so constructed as to guarantee an equally distributed laminar flow over the whole cell cross section. At some height $h$ above $F_1$ the cell is closed by a second screen $F_2$ which filters the liquid and prevents the removal of undissolved particles. The liquid (water, gastric, or intestinal juice) is pumped through the cell by means of a metering pump $P_1$ from a reservoir $R$, after having passed the heat exchanger $H$ for temperature control. The eluate leaving the cell is analyzed for drug content, either continuously or at fixed intervals.

In this model the following external parameters determine the dissolution kinetics: volumetric flow rate, $Q$(cm.$^3$/min.); cross-sectional cell area, $A$ (cm.$^2$); initial drug amount, $m_0$(g.). Since the drug amount is given by the dosage form itself, there remain only two apparatus parameters which are best presented as mass-specific quantities: liquid velocity, $Q_A = Q/A$ (cm./min.); drug amount per unit cell area, $m_{A,0} = m_0/A$(g./cm.$^2$). These two together determine the degree of agitation in the liquid as well as the elimination of the dissolved drug from the system.

One particular feature should be pointed out; different drug amounts are dissolved under identical conditions whenever the parameters $Q_A$ and $m_{A,0}$ are equal. This means that the dissolution of $N$ tablets, studied simultaneously in a cell with cross section $N \cdot A$ and with a volumetric flow rate of $N \cdot Q$ is the same as the average of $N$ runs of single tablets in a cell with cross section $A$ and volumetric flow rate $Q$.

**Modifications**—The cell and the outlet tubes represent a hold-up volume $V_h$ for the dissolved drug, which corresponds to a lag time

$$t_h = V_h/Q \qquad \text{(Eq. 1)}$$

between the dissolution of the drug and the removal of the solute from the system. This hold-up volume can be chosen freely by means of the cell height $h$ between $F_1$ and $F_2$.

In this model there is no hindrance to the elimination of the dissolved drug from the system, whereas in biological absorption the absorbing membranes may represent a drug-specific resistance to the removal of the material from the site of dissolution. If desired, this resistance can be simulated in the following way: a fraction $x$ of the liquid flow $Q$ through the cell is recirculated by means of a second metering pump $P_2$ (see Fig. 1). This simulates the membrane resistance in a quantitative manner: $x = 0$ means no resistance, and $x = 1$ represents complete hindrance of absorption. Thus, any drug-specific permeability of the membranes can be simulated in very convenient way.

It is to be noted that the fixed-volume method appears to be a borderline case of this generalized model. With a circulation factor $x = 1$ and a large hold-up volume $V_h$ the dissolution kinetics of this model should correspond completely to those obtained in a stirred beaker.

## DISSOLUTION KINETICS

Two types of material must be considered separately, the bed of nondisintegrating granules (*e.g.*, a drug powder or a loosely filled capsule) and the disintegrating tablet. Different dissolution kinetics are likely for these two cases because of the different time variation of the effective exchanging surface area during the dissolution process. In the first case, the initial surface area $S_0$ is determined by the number, size, and shape of the particles. Since volume and surface area are geometrically correlated, the further variation of $S$ is governed by general laws, and the dissolution rate follows a general pattern.

In tablets, on the other hand, the variation of $S$ with time is more complicated. In the first moment of dissolution, $S$ is in the order of a few square centimeters, corresponding to the outer geometrical surface area of the tablet. Owing to the liquid agitation

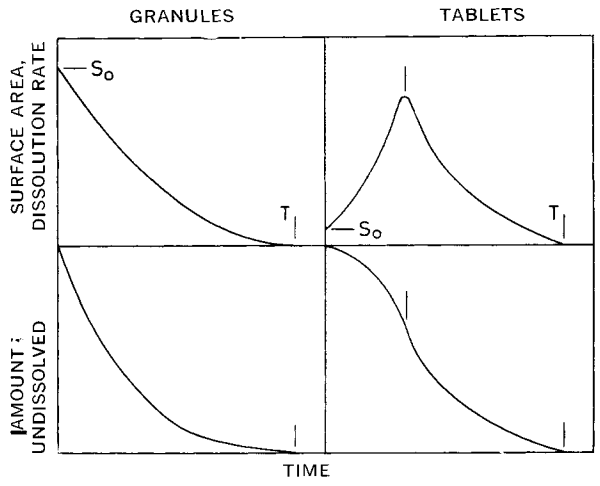


**Figure 2**—*Time variation of surface area* S, *dissolution rate* (dm/dt), *and amount of undissolved drug* m, *for granules and disintegrating tablets (schematically).*

[1] Recently, Baun and Walker [*J. Pharm. Sci.*, **58**, 611(1969)] described a dissolution apparatus very similar to the one proposed in this paper. However, these authors use a fixed liquid volume instead of the continuous flow employed in our method.

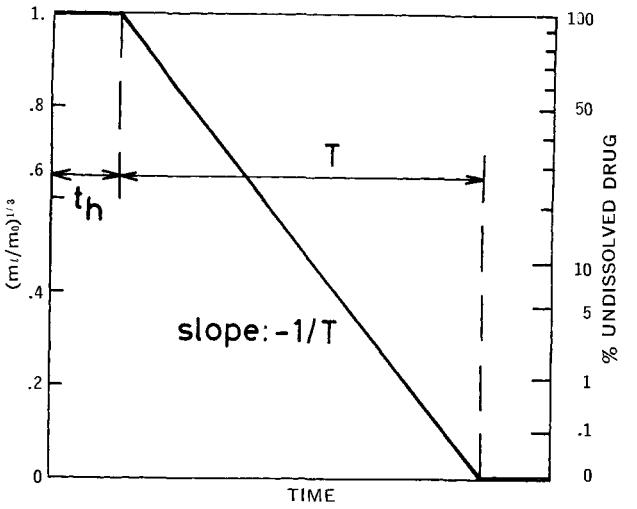


**Figure 3**—*Cube-root dissolution curve of nondisintegrating particles (schematically). Key:* $m_0$, *initial drug amount;* $m_t$, *undissolved amount at time* t; T, *dissolution time;* $t_h$, *lag time.*

and to the action of disintegration adjuvants, the tablet breaks down into fractions, thus resulting in an increase of the total surface area. At the same time the surface of the fractions becomes smaller as a consequence of the dissolution. Consequently, the variation of surface area and dissolution rate is represented by a bell-shaped function, as is shown schematically in Fig. 2. The integral curve, *i.e.*, the amount of undissolved material at time *t*, will be S-shaped, the steepest slope being coincident with the maximum in the $S(t)$ curve.

Although the dissolution kinetics of nondisintegrating granules is of minor importance from a practical point of view, it is of great value for the evaluation of the method itself, since the material-inherent variability is very low and the kinetics can be expressed in general terms.

**Kinetics of Nondisintegrating Granules**[2]—As was first deduced by Noyes and Whitney (14), the dissolution rate-$(dm/dt)$ is related to the effective surface area $S$ of the particles and to the driving force gradient $\Delta c$ by the mass-transfer coefficient

$$k = -(dm/dt)/(S \cdot \Delta c) \qquad \text{(Eq. 2)}$$

Here, $\Delta c$ represents the difference between the saturation concentration $c^*$ and some average concentration in the liquid surrounding the particles. For column-type flow, $\Delta c$ can be expressed in terms of the effluent concentration $c_e$:

$$\Delta c = c^* - c_e/2 \qquad \text{(Eq. 3)}$$

In the special case of nondisintegrating granules of uniform size and shape, the amount of undissolved material $m_t$ varies with time $t$ according to

$$(m_t/m_0)^{1/3} = 1 - t/T \qquad \text{(Eq. 4)}$$

which means that a straight line is obtained when the cube root of the relative undissolved mass is plotted *versus* time (Fig. 3). This dissolution line starts with $(m_t/m_0)^{1/3} = 1$ for $t = 0$, has a slope of $-(1/T)$, and intersects the time axis at $t = T$. Thus, the entire dissolution kinetics is represented by one single constant, the dissolution time $T$, which is the time necessary to dissolve the material completely.

The concentration $c_e$ of the eluate of the cell varies with time in accordance with

$$c_{e,t} = (3m_0/TQ)(1 - t/T)^2 \qquad \text{(Eq. 5)}$$

which means that a plot of the square root of $c_e$ *versus* $t$ results in a straight line. The highest concentration is found at the start:

[2] A list of the notations used and the derivation of the equations is given in the *Appendix*.

**Table I**—Size Parameters of the Benzoic Acid Granules; Fractions *0.26, 0.41, and 0.75* mm.

| | Sieve Screen Limits, mm. | | |
|---|---|---|---|
| | 0.75–1.2 | 0.4–0.75 | 0.2–0.4 |
| Mean spherical particle volume, $V_p(10^{-3}$ cm.$^3)^a$ | *0.81* | *0.13* | *0.013* |
| Equivalent spherical diameter, $D_p$(mm.)$^b$ | 0.75 | 0.41 | 0.26 |
| Mass-specific surface area, $S_m$(cm.$^2$/g.)$^c$ | 63 | 115 | 181 |

[a] Determined by counting a weighed sample of approx. 1000 particles. [b] Calculated as $D_p = (\pi V_p/6)^{1/3}$. [c] Calculated as $S_m = 6/(\rho_p D_p)$.

$$c_{e,0} = 3m_0/(TQ) \qquad \text{(Eq. 6)}$$

**Dependence of T on External Parameters**—The dissolution time $T$ is related to the material and apparatus parameters by the equation

$$T = (D_{p,0}\rho_p)/(2k\Delta c) \qquad \text{(Eq. 7)}$$

Thus, the particle diameter, the amount of material, and the liquid velocity are likely to have an influence on $T$. To express this correlation, two dimensionless quantities are introduced (9, 11, 15), the Reynolds number

$$Re = (Q_A D_p)/\nu \qquad \text{(Eq. 8)}$$

which describes the degree of agitation in the liquid, and the mass-transfer factor

$$j_d \propto k/Q_A \qquad \text{(Eq. 9)}$$

which defines the dissolution rate in a dimensionless way.[3]

The correlation is then of the form

$$j_d \propto (Re)^{-n} \qquad \text{(Eq. 10)}$$

where the exponent $n$ is found to vary between 0.5 and 0.8 for Reynolds numbers between 0.1 and 1 (11, 15). Equation 10 can be rearranged into the form (see *Appendix*)

$$T \propto (Q_A)^{-0.2-0.5} \cdot (D_{p,0})^{1.5-1.8} \qquad \text{(Eq. 11)}$$

which shows the correlation to the experimental parameters $Q_A$ and $D_{p,0}$.

## DISSOLUTION OF BENZOIC ACID GRANULES

### Experimental

**Material**—Granules of benzoic acid were chosen for the basic experiments, since their preparation and assay are very easy and since many data on their dissolution kinetics are available in the literature (7, 9, 11, 16–19). The granules were prepared by the method of Evans and Gerald (9). The reagent grade material was melted and chilled on a flat metal pan. After grinding the granules were screened into three size fractions, the size parameters of which are listed in Table I. To remove fine dust from the particles, they were suspended in distilled water for some hours and, after filtering, dried to constant weight.

**Apparatus**—The dissolution apparatus was used without liquid recirculation ($x = 0$). The dissolution was conducted in deionized water of 25°, which was pumped from a reservoir by means of a metering pump[4] operating at 128 strokes/min. The rate of the pulsating flow was set by means of the stroke amplitude. A Graham condensor connected to a constant-temperature bath was used for temperature control. Two different cells were employed with cross-sectional areas of 2 and 4 cm.$^2$. All other dimensions being exactly

[3] The bed porosity and the Schmidt number, which are also included in the definition of $j_d$, are not taken into consideration since they were constant in these experiments.

[4] LEWA model KH metering pump, LEWA, Leonberg, West Germany; 8-mm. diameter ceramic pumping head.

**Table II**—Dissolution Time $T$, Obtained for Various Combinations of Particle Diameter $D_p$, Liquid Velocity $Q_A$, and Initial Mass Load $m_{A,0}$

| Initial Mass Load, $m_{A,0}$ (mg./cm.²) | Particle Diameter $D_p$ (mm.) 0.26 — $Q_A$ (cm./min.) 2 | 4 | 8 | 16 | 0.41 — $Q_A$ (cm./min.) 2 | 4 | 8 | 16 | 0.75 — $Q_A$ (cm./min.) 2 | 4 | 8 | 16 |
|---|---|---|---|---|---|---|---|---|---|---|---|---|
| | **Dissolution Time $T$ (min.)** | | | | | | | | | | | |
| 31.25 | 47 | 33 | 30 | 30 | 99 | 74 | 74 | 52 | 300 | 227 | 159 | 112 |
| | 49 | 36 | 31 | 34 | 100 | 88 | 93 | 70 | 305 | 230 | 192 | 130 |
| 62.5 | 45 | 36 | 30 | 27 | 102 | 80 | 59 | 51 | 244 | 167 | 132 | 109 |
| | | 37[a] | | | | 82 | | | | 154 | 142 | |
| 125.0 | 57[a] | 39 | 35 | 28 | 114 | 82 | 65 | 54 | 244 | 172 | 143 | 111 |
| | 57 | 45[a] | 37[a] | 29[a] | | 86 | | | | | | |
| | | | | 34 | | 90[a] | | | | | | |
| 250.0 | [81][b] | [53[a]][b] | 41 | 30 | 137 | 100 | 74 | 58 | 264 | 182 | 145 | 115 |
| | | [58][b] | | | | | | | | 208 | | |
| Reynolds number, *Re* | 0.10 | 0.19 | 0.39 | 0.77 | 0.15 | 0.31 | 0.61 | 1.22 | 0.28 | 0.56 | 1.12 | 2.23 |

[a] These values were obtained with the 2-cm.² cell, all others with the 4-cm.² one. [b] Values obtained from nonlinear dissolution curves.

equal, the 4-cm.² cell is shown in Fig. 4. Glass beads 1 mm. in diameter were used as inlet filter $F_1$, on top of which the granules were placed. The upper filter $F_2$ was also a bed of glass beads, held in place by means of a 40-US-mesh stainless steel sieve mounted on a Teflon ring. The hold-up volume of the two cells was 8.8 and 17.6 cm.³, respectively

In order to achieve complete wetting of the granules, 1 cm.³ of a 1% sodium laurylsulfate solution was added per each 0.1 g. of benzoic acid just at the moment when the water reached the granules. After this the cell was closed immediately.

Assay—The solution leaving the cell was collected over fixed time intervals (3, 5, 7.5, 10, 15. . .min.) and titrated with 0.1 or 0.04 $N$ NaOH to a phenolphthalein end point. After completion of each run (30 to 90 min.) the cell was dismantled and rinsed with methanol, the residue of the benzoic acid being titrated for control.

## Results and Discussion

The whole experiment was conducted in the form of a 3 × 4 × 4-factorial design, the three factors being at equal or nearly equal distance from one another on a logarithmic scale: particle diameter, $D_{p,0}$: 0.26, 0.41, 0.75 mm.; liquid velocity, $Q_A$: 2, 4, 8, 16 cm./min.; initial mass load, $m_{A,0}$: 0.031, 0.063, 0.125, 0.250 g./cm.². The results, *i.e.*, the dissolution time $T$ obtained for the various combinations of the three factors, are given in *Table II*(see also *Fig. 7*).

**Shape of the Dissolution Curves**—In almost all experiments a straight line was obtained for the plot of $(m_t/m_0)^{1/3}$ *versus* time, in accordance with the cube root law (Eq. 4). Typical curves are shown in Fig. 5. A lag time between 0.28 and 2.2 min. is seen at the beginning, according to Eq. 1. In general, the points follow the straight line from the start down to ordinate values between 0.5 and 0.6, corresponding to at least 80 to 90% of dissolution. Thus, it is justified to extrapolate the linear part to the time axis to obtain the dissolution time $T$. The upward curved "tail" is due to changes in the geometrical form of the particles and to enlarged bed porosity (floating), which occurs when most of the material has been dissolved.

In a few experiments involving large amounts of the finest (0.26 mm.) particles under low liquid velocities, the dissolution curves do not follow the cube root law. Examples are shown in Fig. 6. This is due to saturation of the liquid, and is discussed in more detail below. In Table II, the $T$ values obtained from nonlinear curves are enclosed in brackets.

**Reproducibility of the Method**—For statistical analysis, the data of Table II are used as logarithms, since Eq. 11 suggests that in this form the effects of the factors are additive and linear. From the 21 duplicate and 2 triplicate determinations, a joint estimate of the method variance can be obtained on the assumption of equal variance for all parameter combinations. The common standard deviation is calculated as ±0.037 for log $T$, corresponding to ±9% in $T$. This includes the variability due to the two different cells.

**Cell Cross Section**—The seven determinations shown in Table II, in which both cells with $A$ = 2 and 4 cm.² are employed, demonstrate the fact that the cell cross section has no influence on the dissolution time, when $Q_A$ and $m_{A,0}$ are kept constant. Statistical analysis of the paired differences between both cells shows the $T$ values of the small cell to be only 2% higher, on the average, which is not significant at all.

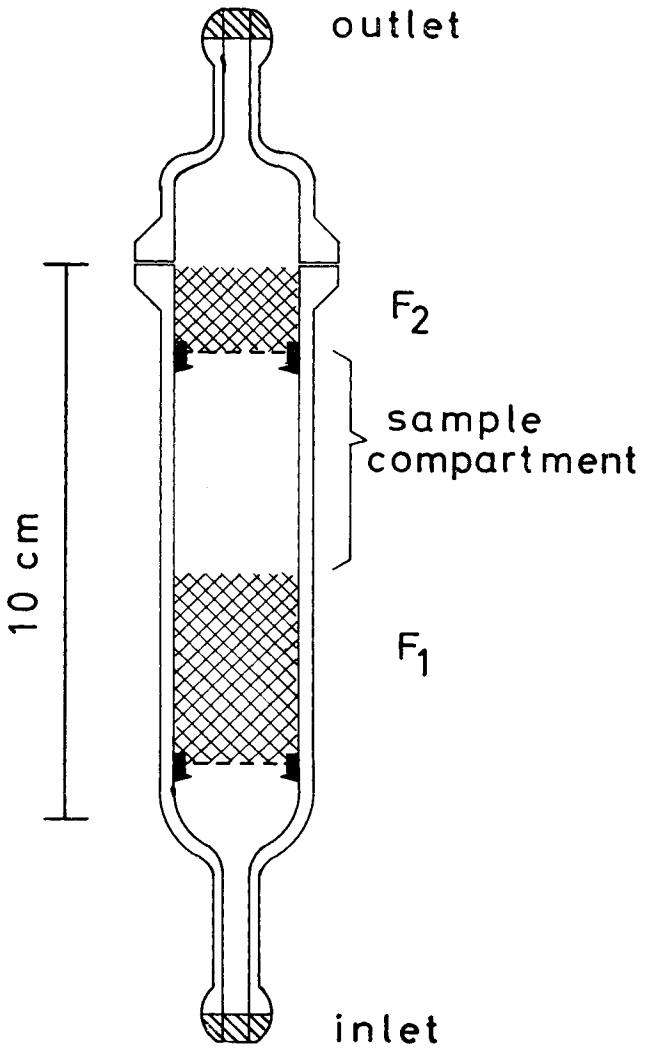


**Figure 4**—*Specifications for the 4-cm.² dissolution cell (drawn to scale). Inner cell diameter 22.6 mm. Height of sample compartment 40 mm.* $F_1$*: stainless steel sieve with 30-mm. bed of glass beads 1 mm. in diameter.* $F_2$*: 40 (US) mesh stainless steel sieve with glass beads.*

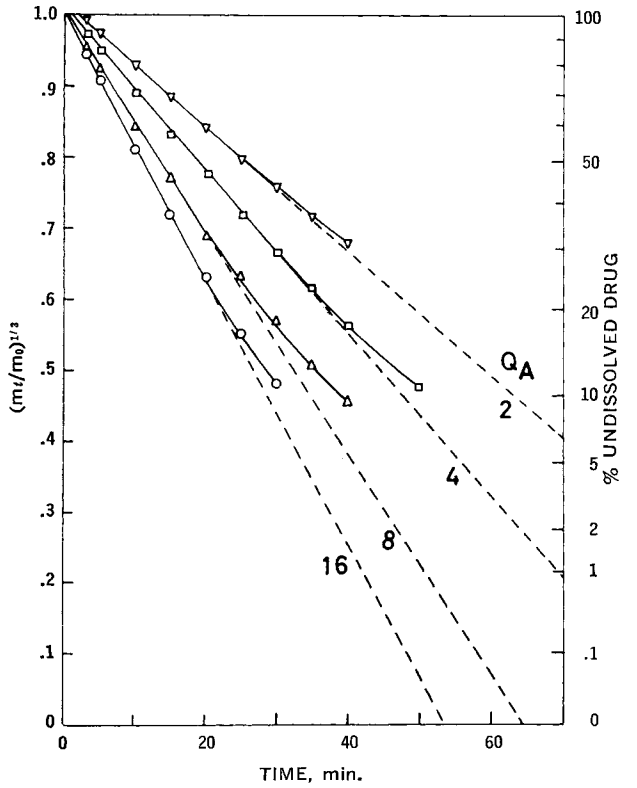


**Figure 5**—*Cube root dissolution curves obtained with benzoic acid granules in water at various liquid velocities* $Q_A$ *(cm/min). Particle diameter,* $D_p$ *= 0.41 mm.; initial mass load,* $m_{A,0}$ *= 125 mg./cm.*$^2$.

**Influence of $D_p$, $Q_A$, and $m_{A,0}$ on the Dissolution Time T**—The influence of these parameters was treated in a quantitative manner by calculating the multiple regression of the logarithms on log $T$, including the linear, quadratic, and mixed second-order terms.[5] The following regression equation is obtained

$$\begin{aligned}\tau = -7.70 &+ 5.67\delta + 0.54\gamma + 0.16\mu \\ &- 0.61\delta^2 + 0.11\gamma^2 + 0.29\mu^2 \\ &- 0.30\delta\gamma - 0.13\gamma\mu - 0.44\mu\delta\end{aligned} \qquad \text{(Eq. 12)}$$

where $\tau$, $\delta$, $\gamma$, and $\mu$ denote the logarithm of $T$, $D_p$, $Q_A$, and $m_{A,0}$, respectively. This model leads to a residual standard deviation of $\pm 0.039$ for $\tau$, which agrees with the value obtained from the replicate determinations alone.

In Fig. 7 the curves are drawn according to a simpler regression model which was obtained by means of a stepwise calculation. This model accounts only for the most significant parameters, namely $\delta$, $\delta^2$, $\gamma^2$, and $\delta\gamma$, and results in a residual standard deviation of $\pm 0.052$ ($\sim \pm 13\%$).

In order to compare these results with Eq. 11, the partial derivatives are calculated from Eq. 12. These are

$$\begin{aligned}\partial\tau/\partial\delta &= 1.45 \\ \partial\tau/\partial\gamma &= -0.31 \\ \partial\tau/\partial\mu &= 0.00\end{aligned} \qquad \text{(Eq. 13)}$$

for the grand average of all observations, *i.e.*, $D_p$ = 0.43 mm., $Q_A$ = 5.67 cm./min., and $m_{A,0}$ = 0.088 g./cm.$^2$. This is equivalent to the equation

$$T \propto (Q_A)^{-0.31} \cdot (D_{p,0})^{1.45} \qquad \text{(Eq. 14)}$$

and is in good agreement with Eq 11.

According to the nonlinear terms in Eq. 12 the exponents in Eq. 14 are different for different combinations of the three parameters. The most important factors contributing to this variation are:

1. Whereas the 0.75-mm. granules have a cubic form which corresponds to a form factor $\kappa = 6$, the two finer size fractions have more elongated granules for which a larger form factor should be used.

2. For higher liquid velocities the granule bed is gradually expanded, *i.e.*, the porosity increases. This reflects the transition from fixed to fluidized bed conditions and results in the flattening of the $\tau(\gamma)$ curves at high flow rates (see Fig. 7).

3. With low initial amounts ($m_{A,0}$ = 31.3 mg./cm.$^2$) the cell cross section cannot be covered uniformly, especially in the case of coarse particles. There are "holes" in the granule layer, through which the liquid flows preferably, thus leaving the granules in a dead zone of flow. As a result, the dissolution time $T$ is, in general, enhanced for these low amounts.

4. For high mass loads, in connection with small granules and low liquid velocities, the liquid becomes more concentrated, and the driving force gradient $\Delta c$ is smaller than the value corresponding to the cube root law (see the discussion in the *Appendix*). Deviations from linearity are observed in this case (see Fig. 6), and the dissolution time is enhanced.

**Influence of Wetting Agent**—As mentioned above, sodium laurylsulfate (NaLS) was added to the liquid at the beginning of the dissolution, in order to improve the wettability of the granules. The influence of a lowered surface tension is of some practical importance, since the surface tension of human gastric juice is known to be of the order of 35 to 50 dyne/cm. (20), a value reached by most aqueous surfactant solutions at and above the critical micelle concentration (CMC). Some experiments involving various single NaLS doses at the start or NaLS solutions of various concentration as solvent liquid, are shown in Table III. It is seen that the initial addition of 1 mg. NaLS per 250 mg. benzoic acid brings the dissolution time to the reproducible and typical value of 37 min., which is not further affected by doses up to 50 mg. Also, use of a 0.01 or 0.1% NaLS solution as solvent does not affect the dissolution time. Only with the 1% solution is $T$ significantly reduced by approximately 20%.

This is consistent with results reported by Parrott and Sharma (19), who found that the solubility of benzoic acid in 1% NaLS solution is higher than in pure water by approximately 15%, owing

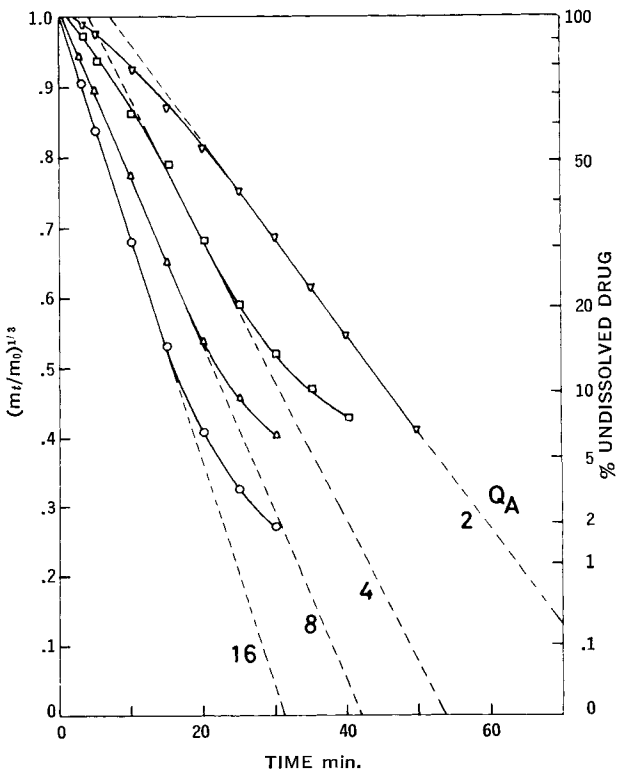


**Figure 6**—*Deviations from cube root law observed with high particle surface area. Particle diameter,* $D_p$ *= 0.26 mm.; initial mass load,* $m_{A,0}$ *= 250 mg./cm.*$^2$*; liquid velocity,* $Q_A$ *from 2 to 16 cm./min.*

[5] The calculation was done on a Univac III digital computer by means of a standard program for multiple regression analysis.

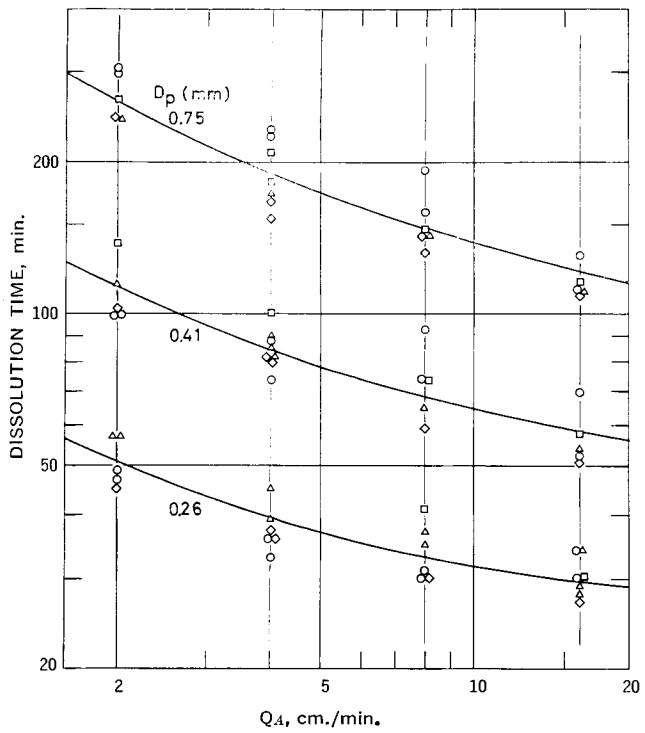


**Figure 7**—*Log-log plot of the correlation between liquid velocity* $Q_A$ *and dissolution time* T *for various particle diameters* $D_p$ *and initial mass loads* $m_{A,0}$. *Key:* ○, *31.3;* ◊, *62.5;* △, *125;* □, *250 mg./cm.*$^2$.

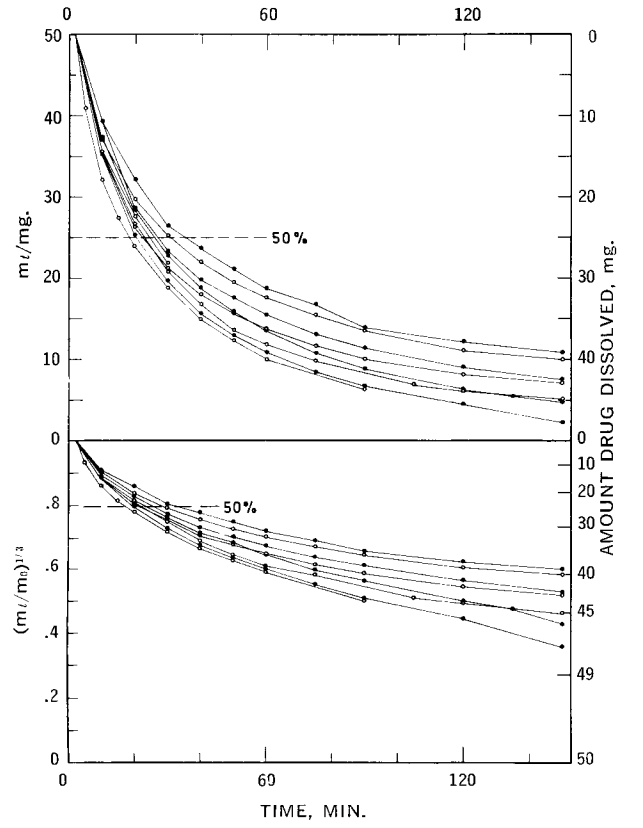


**Figure 8**—*Dissolution of hydrochlorothiazide tablets in artificial gastric juice at 37°. Linear (upper part) and cube root plot (lower part). Two tablets of 25 mg. employed in each run. Cell area,* A = *4 cm.*$^2$*; liquid velocity,* $Q_A$ = *4 cm./min.; initial mass load,* $m_{A,0}$ = *12.5 mg./cm.*$^2$.

**Table III**—Effect of Sodium Laurylsulfate Addition on the Dissolution Time[a]

| % NaLS in Liquid | Surface Tension,[b] dynes/cm. | Single NaLS Dose, mg. | Dissolution Time $T$, min. |
|---|---|---|---|
| 0 | | 0 | 210 |
| 0 | | 1 | 38.0 |
| 0 | | 2 | 36.6 |
| 0 | 72 | 5 | 34.9 |
| 0 | | 10 | 36.4 |
| 0 | | 20 | 34.6 |
| 0 | | 50 | 36.0 |
| 0.01 | 71 | 1 | 35.4 |
| 0.10 | 68 | 1 | 38.1 |
| 1.00 | 52 | 1 | 27.0 |

[a] Experimental conditions: $A$ = 4 cm.$^2$, $D_p$ = 0.26 mm., $Q_A$ = 4 cm./min., $m_{A,0}$ = 0.063 g./cm.$^2$.[b] Lit. (21).

to micellar solubilization. It also agrees with the value of the CMC which is $8 \times 10^{-3}$ mole/l. $\doteq$ 0.23% w/w, at 25° (21). It should be noted that with suitable nonionic surfactants lower concentrations would be sufficient to reduce the surface tension: with polysorbate 80, the CMC of which is 0.001% (22), a 0.05% solution would exhibit the same surface tension as natural gastric juice (20).

## EXAMPLE OF A DISINTEGRATING TABLET

As work on actual tablet formulations is in progress, only one example will be presented in Fig. 8: the dissolution of 25-mg. hydrochlorothiazide tablets, conducted in artificial gastric juice (0.292% HCl, 0.20% NaCl) of 37° without addition of wetting agent, is given in the cube root form as well as in the usual form of $m_t$ *versus* time. The invalidity of the cube root law in this case is seen immediately. No dissolution time $T$ being defined, the dissolution kinetics are best characterized by the $t_{50}$, *i.e.*, the time necessary for 50% dissolution (higher time intervals, *e.g.*, $t_{90}$, are too much affected by dosage variability and thus give no real picture of the dissolution). An average of 25.4 min. is obtained, with a standard deviation of ±5.2 min. (±20%). This shows that, in this special case, the variation between tablets is of the same order of magnitude as the method variation.

## CONCLUSIONS

Theoretical considerations, together with the results obtained from the dissolution of benzoic acid granules, demonstrate the usefulness of the column method for the investigation of dissolution kinetics. The main features may be summarized as follows:

1. Only two apparatus parameters are essential to the dissolution process: the liquid velocity and the mass-specific cell area. These are defined by the volumetric flow rate and the cell diameter, which are both easy to standardize.
2. The method reproducibility is good, as is demonstrated by the ±9% standard deviation in case of homogeneous granules.
3. Arbitrary parameters such as liquid volume, nature of organic solvents or adsorbents, which have to be defined separately for each new drug or dosage, are completely avoided.
4. Scaling-up according to different tablet numbers or dosages is achieved correctly by keeping $m_{A,0}$ and $Q_A$ constant. This was checked by means of two different cells.
5. For uniform-size granules, the theoretically derived cube root was confirmed, and the influence of particle diameter, liquid velocity, and initial mass load was found to agree well with literature data. It is therefore likely that correct and meaningful dissolution data will also be obtained in the case of disintegrating tablets. This will mainly be due to the fact that no concentration buildup occurs in the liquid.
6. Change of the solvent medium, *e.g.*, from gastric to intestinal juice is achieved without difficulty. Also, assay automatization is easily accomplished.

The column-type method thus offers certain advantages over the

various beaker methods with regard to simplicity and reproducibility.

## APPENDIX

*Notation Used*—Values enclosed in brackets refer to the system benzoic acid–water.

$A$ = cell cross-sectional area, cm.$^2$
$c_e$ = drug concentration in the effluent liquid, g./cm.$^3$
$c^*$ = saturation concentration [0.0034], g./cm.$^3$
$\Delta c$ = driving-force concentration gradient, g./cm.$^3$
$D_p$ = equivalent spherical particle diameter, cm.
$j_d$ = mass-transfer factor
$k$ = mass-transfer coefficient, cm./min.
$\kappa$ = geometrical form factor
$m$ = mass of material in the granule bed, g.
$m_A$ = $m/A$, mass of material per unit cell area, g./cm.$^2$
$m_e$ = dissolved amount of material, g.
$m_p$ = mass of single particle, g.
$n$ = exponent of Reynolds number
$\nu$ = kinematic liquid viscosity [0.538], cm.$^2$/min.
$Q$ = volumetric flow rate of liquid, cm.$^3$/min.
$Q_A$ = $Q/A$, liquid velocity, cm./min.
$\rho$ = liquid density [1.000], g./cm.$^3$
$\rho_p$ = particle density [1.266], g./cm.$^3$
$S$ = effective surface area of particle bed, cm.$^2$
$S_w$ = effective surface area per unit mass, cm.$^2$/g.
$t$ = time, min.
$t_h$ = lag time, min.
$T$ = dissolution time from cube root law, min.
$V$ = liquid volume, cm.$^3$
$V_h$ = cell hold-up volume, cm.$^3$
$V_p$ = mean spherical particle volume, cm.$^3$
$Re$ = Reynolds number

Subscripts:

0 = initial value for time zero
$t$ = value at time $t$

**Derivation of Eq. 2**—The driving-force concentration gradient $\Delta c$ is defined as the difference between the saturation concentration $c^*$ and some average concentration actually present in the liquid passing through the particle bed. For column flow conditions $\Delta c$ is given as (11, 15)

$$\Delta c = \frac{c_e}{\ln[1/(1 - c_e/c^*)]} \qquad \text{(Eq. 15)}$$

where $c_e$ denotes the concentration in the liquid leaving the top of the cell. This can be expanded into a power series

$$\Delta c = c^*[1 - c_e/2c^* + \ldots] \qquad \text{(Eq. 16)}$$

This corresponds to

$$\Delta c = c^* \qquad \text{(Eq. 17)}$$

and

$$\Delta c = c^* - c_e/2 \qquad \text{(Eq. 2)}$$

in the zero and first approximation.

In Table IV, the two approximations are compared with the exact values. It is seen that Eq. 17 can be used for low effluent concentrations $c_e/c^* < 0.2$, whereas Eq. 2 extends up to approximately 70% of saturation, the error introduced being less than 10%.

**Derivation of Eqs. 3 and 4**—With particles of uniform size and shape, the surface area $S$ of the particle bed and its mass $m$ are related by the geometrical form factor

$$\kappa = D_p\rho_p(S/m) \qquad \text{(Eq. 18)}$$

At any time of the dissolution process, particle diameter, surface area, and mass are correlated through the equations

$$S_t/S_0 = D_{p,t}^2/D_{p,0}^2 \qquad \text{(Eq. 19)}$$

$$m_t/m_0 = D_{p,t}^3/D_{p,0}^3 \qquad \text{(Eq. 20)}$$

**Table IV**—Driving-Force Concentration Gradient, as Calculated in Various Approximations[a]

| $c_e/c^*$ | Zeroth Approx. (Eq. 17) | First Approx. (Eq. 2) | Exact (Eq. 15) |
|---|---|---|---|
| 0.01 | 1.000 | 0.995 | 0.996 |
| 0.02 | 1.000 | 0.990 | 0.991 |
| 0.05 | 1.000 | 0.975 | 0.976 |
| 0.10 | 1.000 | 0.950 | 0.950 |
| 0.20 | 1.000 | 0.900 | 0.897 |
| 0.30 | 1.000 | 0.850 | 0.842 |
| 0.40 | 1.000 | 0.800 | 0.783 |
| 0.50 | 1.000 | 0.750 | 0.722 |
| 0.60 | 1.000 | 0.700 | 0.655 |
| 0.70 | 1.000 | 0.650 | 0.582 |
| 0.80 | 1.000 | 0.600 | 0.498 |
| 0.90 | 1.000 | 0.550 | 0.391 |
| 1.00 | 1.000 | 0.500 | 0.000 |

[a] $c^*$ assumed to be 1.000.

By substitution of Eqs. 18–20 into the fundamental dissolution Eq. 2 one obtains the following expression for the dissolution rate at time $t$

$$-(dm/dt)_t = (k\kappa m_0^{1/3}m_t^{2/3})/(\rho_p D_{p,0}) \qquad \text{(Eq. 21)}$$

The time-independent quantities can be collected into

$$T = (3D_{p,0}\rho_p)/(k\kappa\Delta c) \qquad \text{(Eq. 22)}$$

In the case of cubic or spherical particles, where $\kappa = 6$ this reduces to

$$T = (D_{p,0}\rho_p)/(2k\Delta c) \qquad \text{(Eq. 4)}$$

With this abbreviation, Eq. 21 is written as

$$-(dm/dt)_t = 3m_0^{1/3}m_t^{2/3}/T \qquad \text{(Eq. 23)}$$

This can be integrated with respect to $dm$ and $dt$, which gives

$$m_t^{1/3} = -(m_0^{1/3}/T)t + C \qquad \text{(Eq. 24)}$$

The integration constant $C$ is determined by the initial condition $m_t = m_0$ for $t = 0$. Hence

$$(m_t/m_0)^{1/3} = 1 - t/T \qquad \text{(Eq. 3)}$$

The integration requires that all parameters included in the dissolution time $T$ are constant throughout the dissolution process. For $\Delta c$, this is true only for sufficiently low effluent concentrations, as long as the approximation Eq. 17 is valid (see Table IV). Whenever the effective surface area of the particle bed is too large, the effluent concentration in the beginning will be more than 10 or 20% of saturation, and deviations from the cube root law are likely.

**Derivation of Eqs. 5 and 6**—The effluent concentration $c_e$ is related to the dissolution rate by

$$c_e = -(dm/dt)/Q \qquad \text{(Eq. 25)}$$

Differentiation of Eq. 3 with respect to $t$ gives

$$(dm/dt)_t = -(3m_0/T)(1 - t/T)^2 \qquad \text{(Eq. 26)}$$

If this is substituted into Eq. 25, one immediately obtains Eq. 5 and, for $t = 0$, Eq. 6

**Deviation of Eq. 11**—From Eq. 7 it follows that

$$T \propto (D_{p,0})/(k) \qquad \text{(Eq. 27)}$$

Stepwise substitution of Eqs. 9, 10, and 8 results in

$$T \propto (D_{p,0})/(j_d Q_A)$$
$$\propto (D_{p,0})(Re)^n/(Q_A)$$
$$\propto (D_{p,0})^{n+1}(Q_A)^{n-1}$$

Insertion of the literature value 0.5 to 0.8 for $n$ gives the form of Eq. 11.

## REFERENCES


(1) G. Levy and B. A. Hayes, *New Engl. J. Med.*, **262,** 1053 (1960).

(2) E. Marlowe and R. F. Shangraw, *J. Pharm. Sci.*, **56,** 498 (1967).

(3) W. E. Hamlin, E. Nelson, B. E. Ballard, and J. G. Wagner, *ibid.*, **51,** 432(1962).

(4) D. Cook, H. S. Chang, and C. A. Mainville, *Can. J. Pharm. Sci.*, **1,** 69(1966).

(5) R. O. Searl and M. Pernarowski, *Can. Med. Assoc. J.*, **96,** 1513(1967).

(6) B. Katchen and S. Symchowicz, *J. Pharm. Sci.*, **56,** 1108 (1967).

(7) M. Gibaldi and S. Feldman, *ibid.*, **56,** 1238(1967).

(8) D. E. Wurster and G. P. Polli, *ibid.*, **50,** 403(1961).

(9) G. C. Evans and C. F. Gerald, *Chem. Eng. Progr.*, **49,** 135 (1953).

(10) J. C. Chu, J. Kalil, and W. A. Wetteroth, *ibid.*, **49,** 141 (1953).

(11) C. E. Dryden, D. A. Strang, and A. E. Withrow, *ibid.*, **49,** 191(1953).

(12) P. M. Weinspach, *Chem. Ing. Tech.*, **39,** 231(1967).

(13) M. Pernarowski, W. Woo, and R. O. Searl, *J. Pharm. Sci.*, **57,** 1419(1968).

(14) A. A. Noyes and W. R. Whitney, *J. Am. Chem. Soc.*, **19,** 930(1897).

(15) M. Leva, "Fluidization," McGraw-Hill, New York, N. Y., 1959, p. 247.

(16) P. J. Niebergall and J. E. Goyan, *J. Pharm. Sci.*, **52,** 29 (1963).

(17) A. H. Goldberg, M. Gibaldi, J. L. Kanig, and J. Shanker, *ibid.*, **54,** 1722(1965).

(18) H. Nogami, T. Nagai, and K. Ito, *Chem. Pharm. Bull.*, **14,** 351(1966).

(19) E. L. Parrott and V. K. Sharma, *J. Pharm. Sci.*, **56,** 1341 (1967).

(20) P. Finholt and S. Solvang, *ibid.*, **57,** 1322(1968).

(21) S. J. Rehfeld, *J. Phys. Chem.*, **71,** 738(1967).

(22) M. R. Vidal-Paruta and L. D. King, *J. Pharm. Sci.*, **53,** 1217(1964).


## ACKNOWLEDGMENTS AND ADDRESSES


Received on September 16, 1968 from the *Pharmaceutical Development Laboratories, Pharmaceutical Division, CIBA Limited, Basle, Switzerland.*

Accepted for publication July 9, 1969.

The author is indebted to Prof. J. L. Lach and Dr. A. Hunger for valuable discussions and help in preparing the manuscript, and to Dr. K. Mullen for his assistance in the statistical analysis of the results.


# *NOTES*

# Identification of Monomeric and Polymeric 5,7,3′,4′-tetrahydroxyflavan-3,4-diol from Tannin Extract of Wild Cherry Bark USP, *Prunus serotina* Erhart, Family Rosaceae


**LEONARD BUCHALTER**



**Abstract** □ A phytochemical investigation of the tannin content of wild cherry bark USP showed the presence of nonhydrolyzable flavanoidal-type tannins, consisting of monomeric and polymeric leucocyanidin units. Identification was accomplished by paper chromatography, visible and IR spectrophotometry, with commercial samples, and fragmentation by potassium fusion.



**Keyphrases** □ *Prunus serotina*—tannin extract □ 5,7,3′,4′-Tetrahydroxyflavan-3,4-diol, monomeric, polymeric—extraction, identification □ Paper chromatography—separation, identification □ IR, visible spectrophotometry—identity


Many extracts of drugs from plant sources have a reported tannin content. The word tannin is one that may be applied to several distinct chemical entities. Tannins may consist of the hydrolyzable types which are readily hydrolyzed by acids or enzymes and are therefore classified as gallotannins or ellagotannins. Tannins may also consist of monomeric and polymeric flavan 3,4-diol or 3-ol units. This type of tannin is the nonhydrolyzable or condensed tannin. In many cases the exact chemical nature of the reported tannins has not been evaluated. The purpose of this experiment was to evaluate phytochemically the reported tannin content of wild cherry bark USP.

## EXPERIMENTAL

**Materials**—Paper chromatography was carried out in glass tanks on Whatman No. 1 filter paper. Visible spectra were obtained from a spectrophotometer (Beckman DB). IR spectra were made on a spectrophotometer (Beckman IR 8). Commercial samples of cyanidin (K & K Labs, Plainview, N. Y.) were used. Wild cherry bark USP (S. B. Penick Co., New York, N. Y.) was also used.

**Preparation of Extracts**—Five hundred grams of coarse, dried wild cherry bark USP, *Prunus serotina* Erhart, Family Rosaceae, was defatted with successive washings of petroleum ether and chloroform. This defatted material was extracted with equal parts of